



UNIVERSITY OF LEEDS

This is a repository copy of *Tribocorrosion of hard-on-hard total hip replacements with metal and ceramic counterfaces under standard and adverse loading conditions*.

White Rose Research Online URL for this paper:
<http://eprints.whiterose.ac.uk/103351/>

Version: Accepted Version

Article:

Beadling, AR, Bryant, M, Dowson, D et al. (1 more author) (2016) Tribocorrosion of hard-on-hard total hip replacements with metal and ceramic counterfaces under standard and adverse loading conditions. *Tribology International*, 103. pp. 359-367. ISSN 0301-679X

<https://doi.org/10.1016/j.triboint.2016.07.022>

© 2016, Elsevier Ltd. Licensed under the Creative Commons Attribution-NonCommercial-NoDerivatives 4.0 International
<http://creativecommons.org/licenses/by-nc-nd/4.0/>

Reuse

Unless indicated otherwise, fulltext items are protected by copyright with all rights reserved. The copyright exception in section 29 of the Copyright, Designs and Patents Act 1988 allows the making of a single copy solely for the purpose of non-commercial research or private study within the limits of fair dealing. The publisher or other rights-holder may allow further reproduction and re-use of this version - refer to the White Rose Research Online record for this item. Where records identify the publisher as the copyright holder, users can verify any specific terms of use on the publisher's website.

Takedown

If you consider content in White Rose Research Online to be in breach of UK law, please notify us by emailing eprints@whiterose.ac.uk including the URL of the record and the reason for the withdrawal request.



eprints@whiterose.ac.uk
<https://eprints.whiterose.ac.uk/>

Tribocorrosion of Hard-on-Hard Total Hip Replacements with Metal and Ceramic Counterfaces under Standard and Adverse Loading Conditions

Andrew R. Beadling*, Michael Bryant, Duncan Dowson, Anne Neville.

Institute of Functional Surfaces, School of Mechanical Engineering, University of Leeds, Leeds, LS2 9JT, UK

* - a.r.beadling@leeds.ac.uk, corresponding author.

Abstract

28 mm Metal-on-Metal (MoM) and Metal-on-Ceramic (MoC) Total Hip Replacements were articulated to 1 million cycles under both Standard Gait and Microseparation conditions. The hip simulator was fully instrumented with a three-electrode electrochemical cell to facilitate monitoring of corrosive degradation. The estimated volume loss from corrosion at the bearing surface was seen to increase by nearly an order of magnitude for both devices, representing as much as 17 % of total degradation. Anodic current transients also displayed near order of magnitude increases in the peak current for both bearing couples. An adverse loading scenario could cause as much as an order of magnitude increase in the metallic ions released into the joint capsule as well as an increased volume of wear debris.

Keywords: Total Hip Replacement, Tribocorrosion, Hard-on-Hard, Metal Ion Release

1. Introduction

The use of Metal-on-Metal (MoM) total hip replacements (THRs) has taken a rapid downturn in recent years following higher than acceptable failure rates [1]. Initially

promised as a low-wear option, the poor performance has largely been attributed to soft tissue reactions caused by metallic debris and ions released into the joint [2]. Traditionally joint replacement devices are benchmarked against other designs using laboratory simulators, in order to ascertain a rate of material loss during articulation through gravimetric assessment [3]. This wear rate does not necessarily capture all the relevant information regarding the prediction of *in-vivo* performance. Initial simulator studies for Metal-on-Metal devices displayed much lower wear rates compared to the so called 'gold standard' Metal-on-Polymer (MoP) bearings [4–7]. Analysis of the wear debris produced in simulators also seemed to suggest MoM bearings would be less likely to cause wear induced osteolysis and aseptic loosening [8]; both of which are main causes for revision in MoP THRs. These initially promising results from simulator studies lead to MoM devices being targeted as a longer-term solution for younger and more active patients. These results did not translate to good *in-vivo* performance for all patients however.

More recent studies have begun to explore the use of electrochemical analysis of prostheses during hip simulation [9–13]. Most metallic biomaterials form a passive oxide film spontaneously in air which protects the alloy from corrosive degradation [14]. Articulation of a metal surface can damage this film and expose the bulk alloy to the electrolyte, accelerating both mechanical and chemical material loss [15]. Our recent work has shown that the degradation of MoM Total Hip Replacements (THRs) is a complex mix of mechanical and corrosive phenomena [11,12,16]. First proposed by Watson *et al.* [15] in relation to a sliding tribological contact, the total material loss was shown to be able to be expressed as pure wear (W_0), pure corrosion (C_0) and their synergistic effects (S). The synergies can be further broken down to corrosion-enhanced wear (dWc) and wear-enhanced corrosion (dCw), as shown in Equation 1.

$$T = W_0 + C_0 + S \quad (1)$$

$$S = dWc + dCw$$

By utilising a three-electrode electrochemical cell integrated into a hip simulator, shifts in the Open Circuit Potential (OCP) of the THR can provide qualitative information on reactions taking place at the articulating surface [10]. Linear Polarisation Resistance (LPR) measurements have also facilitated measurement of the corrosion current of the device which enables, through Faraday's Law, the material loss due to electrochemical corrosion to be quantified [12,13,17]. This is a direct measure of the current produced resulting from metal ion release at the implant surface. The current increases as more extensive metal/metal contact occurs. Hesketh *et al.* [13] reported a reduction of current for 36mm diameter Metal-on-Metal bearings during the commonly recognised bedding-in phase. This may also be attributed to the formation of a proteinaceous tribofilm on the surface [18,19]. An increased focus on the articulation interface has revealed the importance of these tribochemical reaction layers which form on the metal surface as a result of protein interaction with the surface during sliding [20,21]. The ability to assess how a device with a metal surface will perform in-vivo needs a greater understanding of the interaction between the tribology and electrochemistry. Electrochemical instrumentation can therefore provide valuable insight into the degradation at the tribological interfaces of joint replacements. Such methods provide a quantitative in-situ and in-real time assessment of corrosive material loss.

Of increasing interest within the community is the effect of adverse loading conditions and daily living activities on the degradation of implanted devices. It is becoming recognised that long-term studies under a standard ISO twin-peak cycle [22] are not sufficient to replicate

their daily use *in-vivo*. In addition, some devices may be sensitive to adverse loading conditions such as high inclination angle and/or microseparation.

Microseparation occurs when the centre of rotation of both the femoral head and acetabular cup move relative to each other during a cycle, typically during the 'swing phase.' As illustrated in Figure 1 this can result in a collision when the components re-engage at 'heel strike,' which results in a much more severe contact. Microseparation has been shown to increase the wear rates of 28 mm devices three to four-fold over the first and second million cycles, commonly thought to be a bedding-in period [23,24]. MoM devices were initially marketed as low-wear devices compared to MoP couples, with orders of magnitude lower reported simulator wear rates [4]. A three to four-fold increase in MoM 'wear' may therefore be significant, but is still orders of magnitude lower than typical values reported for MoP devices. Gravimetric wear does not fully capture the failure mechanisms of MoM bearings. There may therefore be a shift in the importance of the degradation mechanisms, and the path to failure for Hard-on-Hard prostheses. It is the aim of this study to examine the electrochemical degradation from the metallic bearing surface of total hip replacements articulating against metal (MoM) and ceramic (MoC) counterfaces under standard and adverse simulation methods.

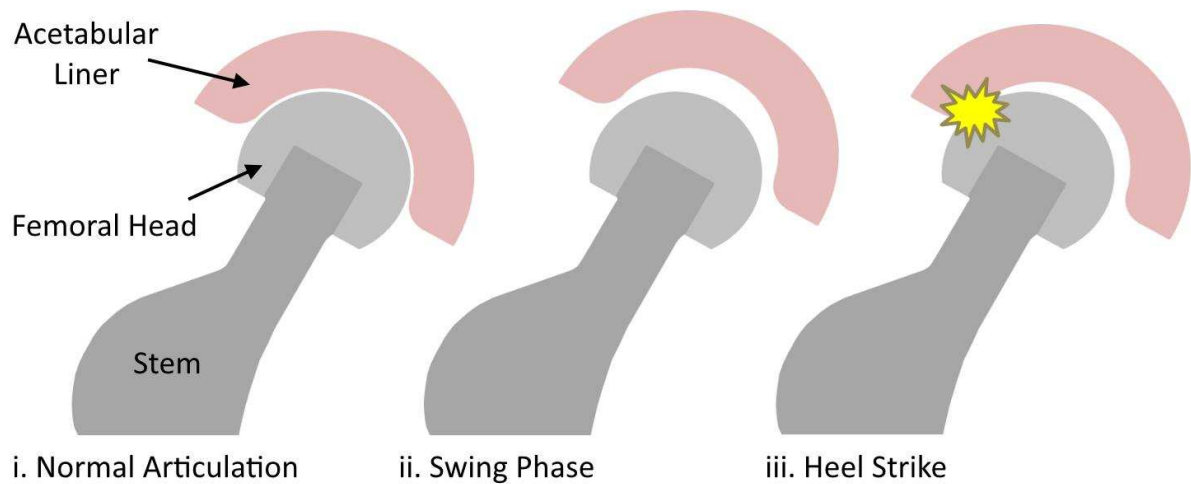


Figure 1 - Schematic Illustration of Microseparation occurring during the 'swing phase' of a walking cycle.

2. Material and Methods

2.1. Hip Simulation

Two 28 mm diameter Hard-on-Hard THR bearing combinations were tested to one million cycles in a ProSim Deep Flexion Hip Simulator (Simulation Solutions, UK). High-Carbon (HC) Cobalt Chromium Molybdenum alloy (CoCrMo) femoral heads were articulated against HC CoCrMo acetabular cups for the Metal-on-Metal combination. For Metal-on-Ceramic (MoC) components from a different manufacturer were used with Low-Carbon (LC) CoCrMo femoral heads articulated against Biolox® delta Aluminum Oxide ceramic cups. An example of the components can be seen in Figure 2.

The MoC couple was selected in order to simplify the contact with only one electrochemically active metallic surface under sliding. In both instances, cups were fixed in place using Ti6Al4V acetabular shells which were cemented into the hip simulator fixture using laboratory grade Poly(Methyl Methacrylate) (PMMA) bone cement. The femoral heads were held in place using a fixture created from high compressive strength resin (Torlon

4203). All other fixtures were made from polyetheretherketone (PEEK) in order to electrically isolate the bearings from the simulator. The bearing combinations were tested to one million cycles at 1 Hz under a twin-peak loading profile detailed in Table 1 [13]:



Figure 2 – Image of unworn 28 mm diameter (left to right) CoCrMo Femoral head, CoCrMo Acetabular Liner and BioloX®delta Ceramic Acetabular Liner.

Table 1 – Twin-peak profile parameters for both Standard Gait and Microseparation Cycles

	Heel-strike & Toe-off Load (N)	Swing Phase Load (N)	Flexion / Extension (°)	Internal / External Rotation (°)	Swing-phase Separation (mm)
Standard Gait (SG)	3,000	300	+30 / -15	±10	-
Microseparation (MS)	3,000	300	+30 / -15	±10	0.8

Two repeats for each condition were conducted giving an ‘n’ value of 2. The microseparation was affected by applying a negative load during the swing phase, limited to 0.8 mm separation of the centres of rotation of each component. The lubricant used was Foetal Bovine Serum (FBS) diluted to 17 gL⁻¹ total protein content [25] with phosphate buffered saline. Sodium Azide (0.03 % w/v) was added in order to retard bacterial growth during the test. Every 333,000 cycles the test was paused in order to change the serum. The

serum was drained and the station was rinsed three times with deionised water before filling again with fresh serum.

2.2. Electrochemistry

The hip simulator was instrumented with a three-electrode electrochemical cell to facilitate *in-situ* measurements of corrosive degradation. For the Metal-on-Metal bearing combination, a connection was made to the rear of the acetabular shell, forming the working electrode (WE). For the Metal-on-Ceramic combination, the working electrode connection was taken from the femoral head, inside the modular taper connection. The working electrode therefore compromised all metallic components which remained in contact and were exposed to the lubricant during sliding. The cell was completed using a combination Silver/Silver Chloride (Ag/AgCl) reference electrode and platinum (Pt) counter electrode. All tests were completed using a PGSTAT101 (Metrohm Autolab, Netherlands) Potentiostat. Care was taken to seal connections and taper junctions with silicone sealant in order to prevent them coming into contact with the lubricant. Any electrochemical measurements should therefore be solely concerned with the sliding interface at the bearing surface. A schematic representation of the hip simulator test cell can be seen in Figure 3.

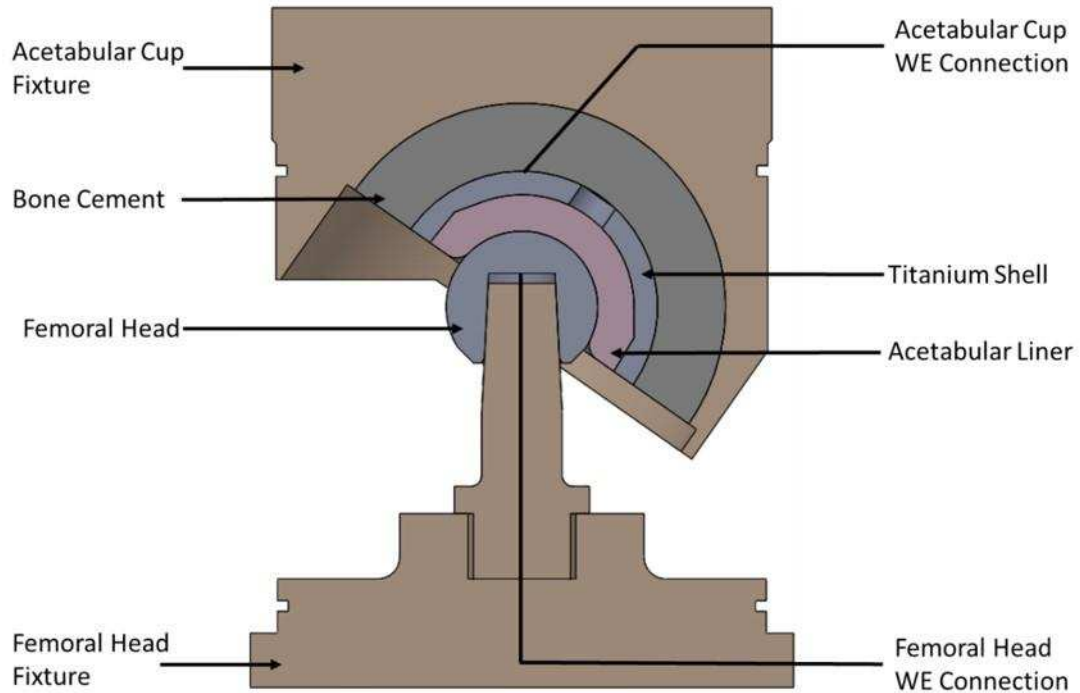


Figure 3 - Schematic representation of the Hip Simulator test cell.

The Open Circuit Potential (OCP) was monitored continuously over the course of each test to give a semi-quantitative assessment of the reactions taking place on the exposed surface of the working electrode. Every 10,000 cycles the resistance to polarisation (R_p) was determined using Linear Polarisation Resistance (LPR, ± 25 mV vs. OCP at 1 mVs^{-1}). Examples of fitted LPR curves to determine the slope and thus R_p can be seen in Figure 4. The corrosion currents (I_{corr}) were estimated using the Stern-Geary equation (Equation 2) [26]. This was done in order to quantify the material degradation as a result of corrosion. The Tafel constants (β_a and β_c) were both assumed to be 120 mV/decade throughout the test as per the qualification set previously by Hesketh *et al.* [12,27].

$$I_{\text{corr}} = \beta_a \beta_c / 2.303 R_p (\beta_a + \beta_c) \quad (2)$$

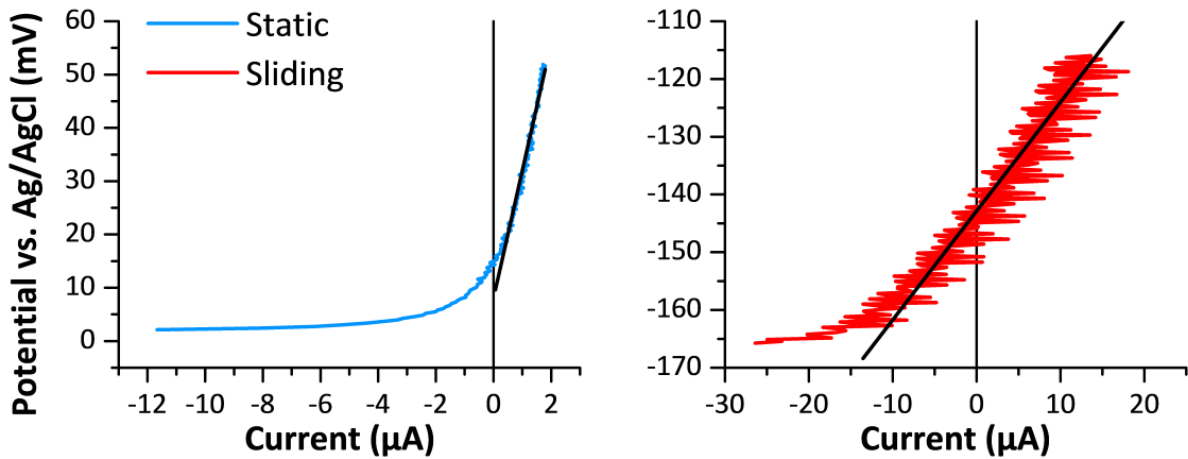


Figure 4 – Example LPR curves for Static and Sliding conditions showing the fitted R_p slope.

Estimates for I_{corr} were then integrated with respect to time in order to give a total charge transfer (Q) (Equation 3). The charge transfer was then used to estimate a mass loss as a result of corrosive phenomena at the working electrode surface using Faraday's Law (Equation 4). Due to the assumptions commonly made for pure metals there is some uncertainty in applying Faraday's Law to an alloy. As CoCrMo has three main constituent elements, each with different molar masses and half-cell valence numbers, interpretation of the data can be critical. A weighted average molar mass (59.2 g/mol) and valence number (2.35) was used based on the approximate percentage alloy composition (Co \approx 62.5 %, Cr \approx 28 %, Mo \approx 6 %). This assumes a stoichiometric release of ions from the working electrode surface, which may not be the case. Upper and lower error bars (shaded regions) in Figures 7 and 8 therefore represent the values for Cobalt (58.9, 2) and Chromium (51.99, 3) respectively, to account for possible preferential release of those elements.

$$Q = \int_0^t I_{corr} dt \quad (3)$$

Where:

Q = Charge Transfer (C)

I_{corr} = Corrosion Current (A)

t = time (s)

$$m = MQ / nF \quad (4)$$

Where:

- m = Mass loss from oxidation
- M = Atomic Mass (g/mol)
- N = Valence number
- F = Faraday's Constant (96,490 C/mole)

Intermittent Potentiostatic Polarisation measurements were taken every 10,000 cycles in between LPR sweeps. The system was polarised to +50 mV with reference to the OCP for 10 seconds and the resultant anodic current transient was sampled at high frequency (100 Hz). An analogue voltage signal was also taken from the hip simulator load cell and sampled at the same rate by the potentiostat. The resultant current was governed by the Butler-Volmer equation (Equation 5) and this enabled monitoring of the depassivation/repassivation kinetics during a cycle in an attempt to link the tribology of the cycle to the electrochemistry.

$$I = I_{corr} \left\{ \exp\left(\frac{\alpha_a n F \eta}{RT}\right) - \exp\left(-\frac{\alpha_c n F \eta}{RT}\right) \right\} \quad (5)$$

Where:

- I = Current as a result of applied potential (A)
- α_a = Anodic charge transfer coefficient
- α_c = Cathodic charge transfer coefficient
- η = Applied overpotential (V)
- R = Ideal Gas Constant
- T = Temperature (Kelvin)

2.3. Total Volume Loss

For the Metal-on-Ceramic series an attempt was made to determine the overall volume loss from the components, in order to estimate the proportion of material loss from the bearing

surface as a result of corrosion. This was not undertaken for the Metal-on-Metal series in order to study the formation of tribofilms on the implant surface, which may have been affected by the cleaning procedure. Two approaches were taken; gravimetric loss and surface form profiling.

For gravimetric assessment, the components were weighed before the test on an analytical balance with ± 0.01 mg precision (Mettler Toledo XPE205) in a controlled atmosphere. After testing the components were subjected to the cleaning regime described in ISO14242-2 [28] and weighed again. Each component was weighed in rotation until five readings within 0.1 mg were obtained. The difference between the two gravimetric points was then taken as the material loss as a result of articulation during the test.

For surface form profiling a sub-micron accurate Coordinate Measuring Machine (CMM, Mitutoyo Legex 322) was used to map the surface by taking single points within 0.5 mm of each other. These points on the surface were used to generate an XYZ coordinate cloud and this was imported into commercially available RedLux Sphere Profiler software. By analysing damage noted on the surface, an estimate for the volume loss during sliding could be made.

3. Results

3.1. Open Circuit Potential (OCP)

Figures 5 and 6 show the OCP trends over one million cycles for Metal-on-Metal and Metal-on-Ceramic bearings respectively. The Metal-on-Metal bearings stabilised to an initial noble potential of approximately -50 to +50 mV for each SG 1 and SG 2 respectively during the settle period. Upon the initiation of sliding under standard gait, this potential immediately shifted cathodically to an initial value of approximately -200 to -300 mV. This cathodic shift is commonly seen in tribocorrosion as a result of the removal of protective surface oxides;

so called “depassivation”. The OCP under standard gait gradually shifted more noble over the course of the experiment, at points almost reaching pre-sliding values, and ending at approximately -200 mV after one million cycles for both implant combinations. Once sliding had stopped a shift in the anodic direction (i.e. more noble) was observed for all Metal-on-Metal bearings, suggesting a decrease in corrosion.

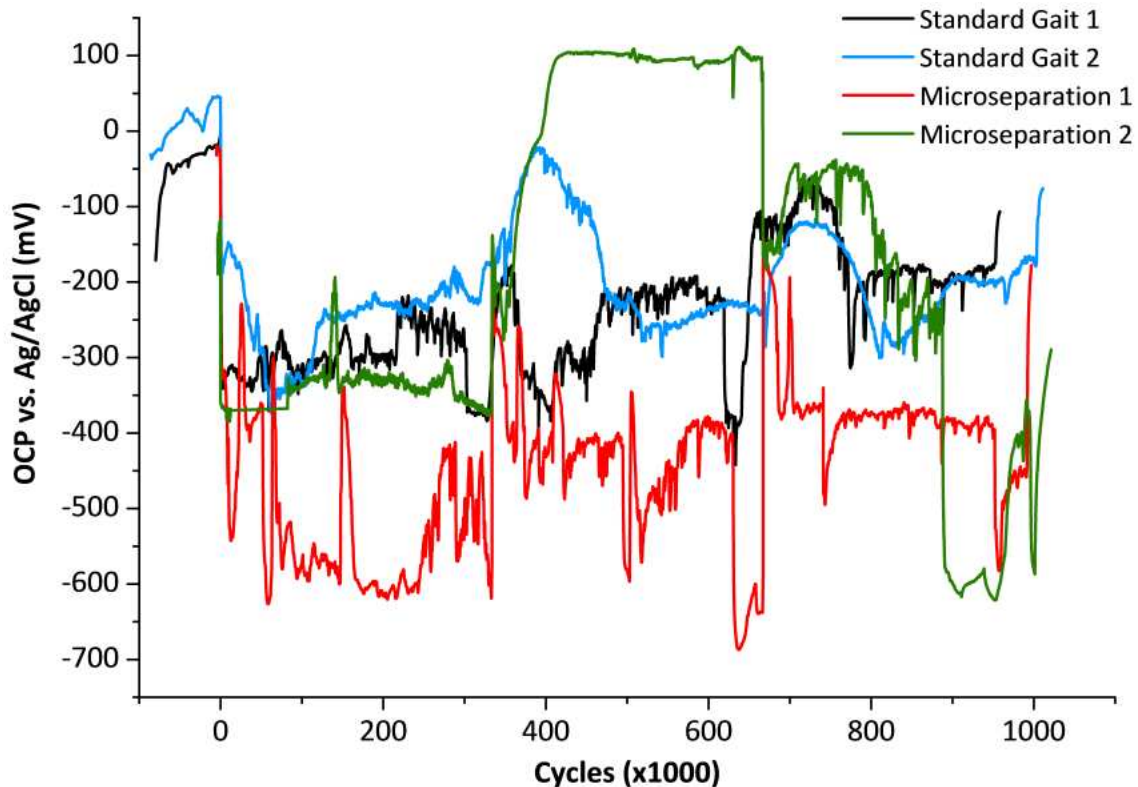


Figure 5 – Open Circuit Potential vs. Ag/AgCl for 28 mm MoM hip joints over one million cycles.

For the MoM bearings under microseparation (Figure 5), one bearing displayed a much greater cathodic shift to approximately -500 mV and remained low throughout the course of the test. This bearing also displayed large spikes and transient behaviour when compared to standard gait. The second bearing subjected to microseparation also displayed transient behaviour although appeared more stable than the first repeat. Upon initiation of sliding this device shifted to approximately -350 mV and remained relatively stable there over the

first 333,000 cycles. After the serum change however the observed OCP was more noble at between approximately -500 and -250 mV. The OCP then began to shift more noble to approximately +100 mV and remained stable there. Upon the second serum change at 666,000 cycles lower OCP values of between -50 and -300 mV were reported and also shifted to as low as -600 mV before the end of the test.

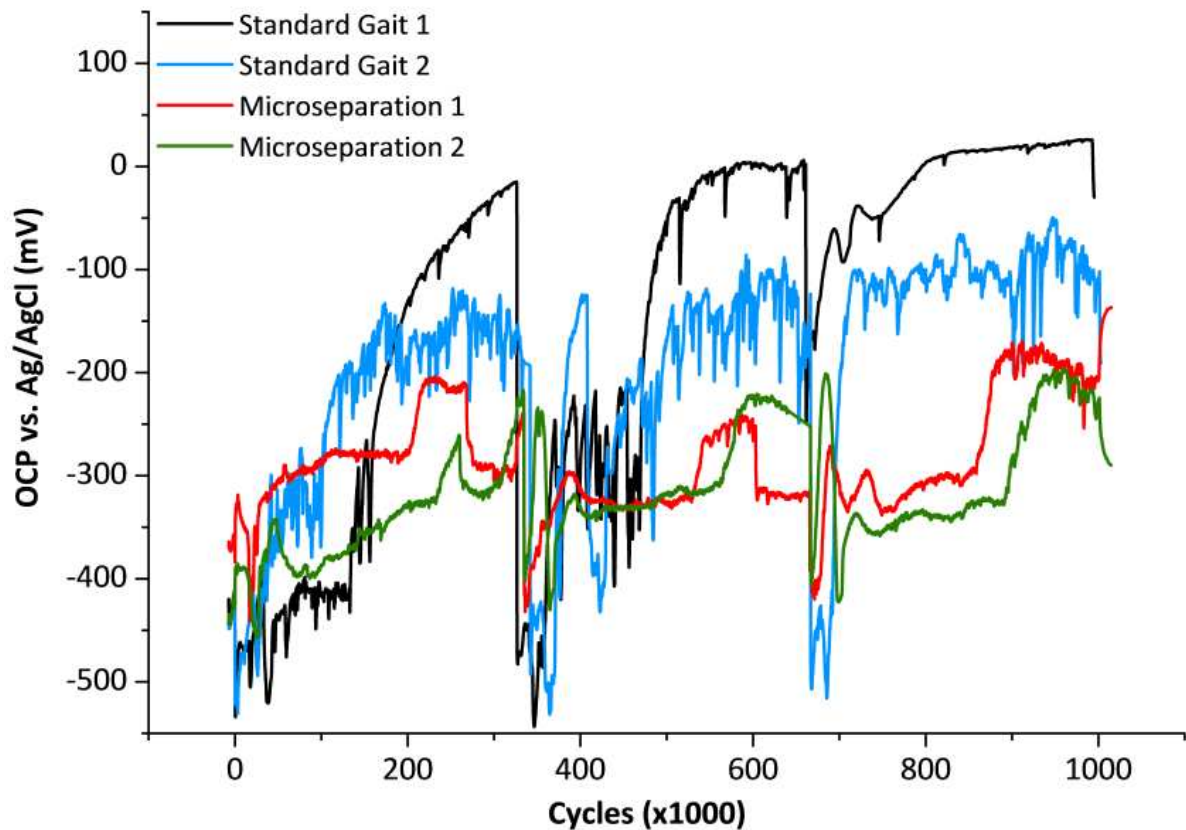


Figure 6 – Open Circuit Potential vs. Ag/AgCl for 28 mm MoC hip joints over one million cycles.

For bearings with a ceramic acetabular cup, shown in Figure 6, the OCP for a standard gait displayed different trends compared to the Metal-on-Metal bearing. All bearings displayed a much more negative initial static potential when compared to MoM devices, of approximately -350 to -450 mV. Upon initiation of sliding there was a small cathodic shift but for standard gait the gradual ennoblement was much more rapid, reaching relatively

noble OCP values of 0 mV for one bearing and approximately -100 mV for the second. This occurred over 333,000 cycles and at serum changes the initial low OCP was restored during a brief static period before sliding. Once sliding was initiated again however the OCP immediately began to shift towards noble values again.

Under microseparation a small cathodic shift in OCP was also noted upon sliding. After this the OCP shifted slightly more noble than pre-sliding values, but remained lower than standard gait over the course of the test between approximately -200 and -350 mV.

3.2. Linear Polarisation Resistance

The cumulative volume loss as a result of corrosion at the bearing surface, estimated from Polarisation Resistance (R_p) and Faraday's Law, can be seen in Figures 7 and 8. For Metal-on-Metal bearings under standard gait the contribution of corrosion to overall material loss during sliding was estimated at 0.029 and 0.056 mm³. The rate of material loss also remained constant over the test.

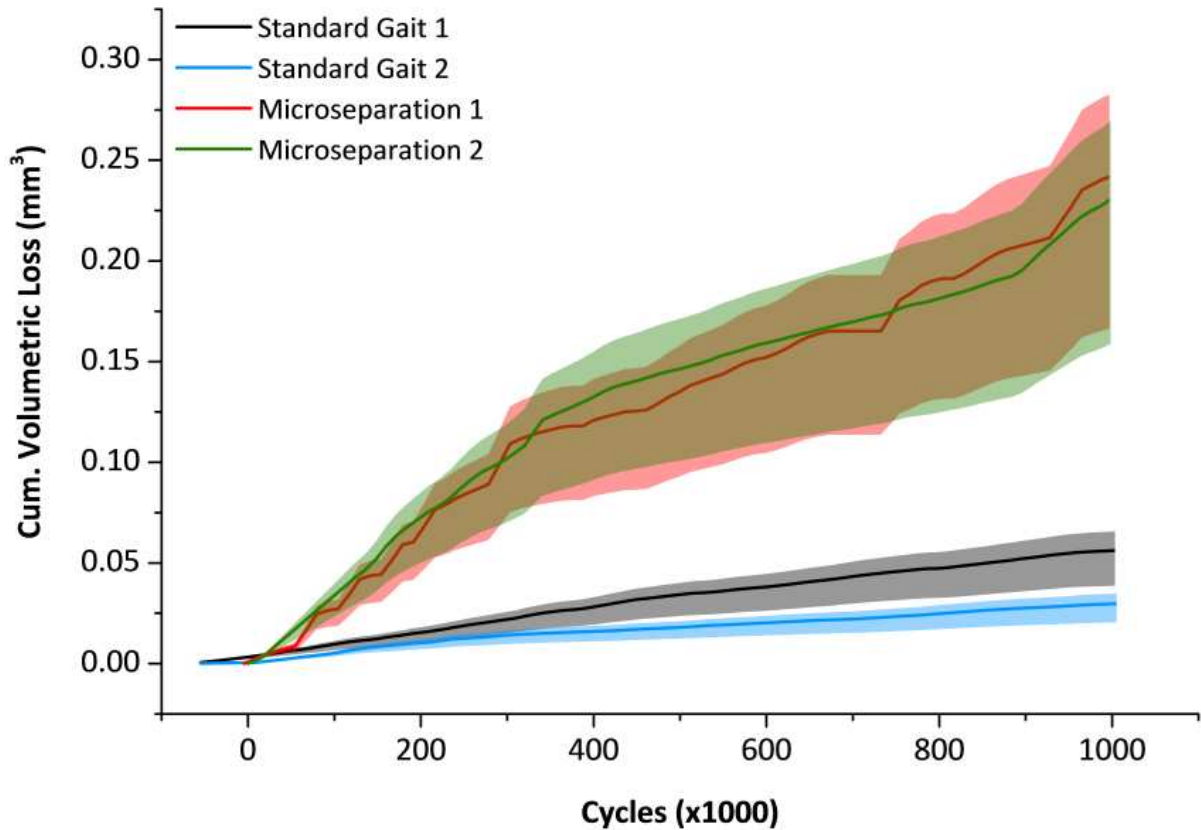


Figure 7 – Estimated cumulative volume loss as a result of corrosion at the bearing surface for 28 mm MoM hip joints over one million cycles. Shaded areas represent possible preferential release of Cobalt or Chromium ions.

Under microseparation the final values for corrosive material loss were found to be much higher at 0.24 and 0.23 mm³. The rate of material loss also changed regularly with the bearing undergoing periods of higher corrosion current (I_{corr}) values, resulting in spikes in the cumulative volume loss. A good overall correlation was noted between the two samples.

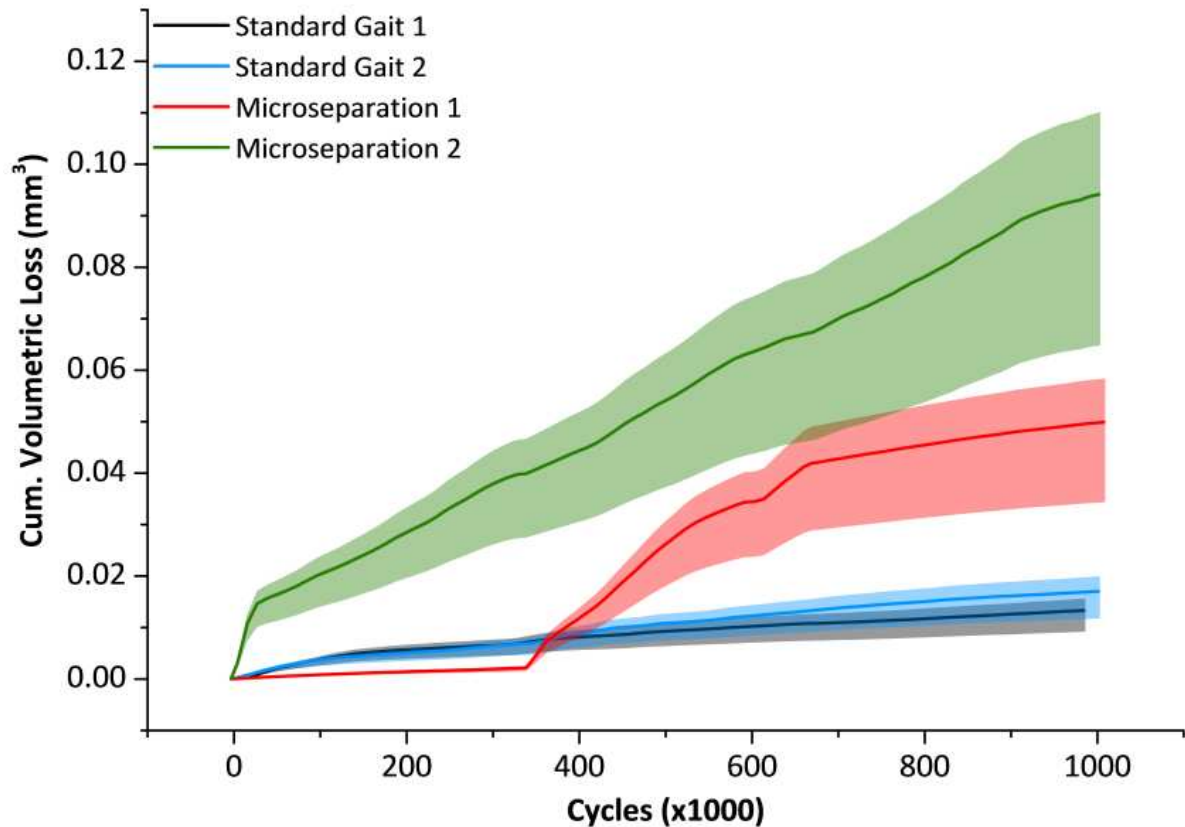


Figure 8 – Estimated cumulative volume loss as a result of corrosion at the bearings surface for 28 mm MoC hip joints over one million cycles. Shaded areas represent possible preferential release of Cobalt or Chromium ions.

For Metal-on-Ceramic bearings, shown in Figure 8, the overall material loss as a result of corrosion was lower than that seen in the Metal-on-Metal devices at 0.013 and 0.017 mm³ under standard gait. Under microseparation the bearings also displayed higher rates of degradation ending at 0.094 and 0.049 mm³. During the first 333,000 cycles one bearing displayed much lower corrosion rates than had been observed under standard gait. This was thought to have been an issue related to the reference/counter electrode used and rates were immediately higher when the serum was changed and the electrode was replaced. The corrosion rates also appeared much more stable under microseparation than had been seen for Metal-on-Metal bearings with more consistent corrosion current values (i_{corr}).

3.3. Anodic Polarisation

Typical anodic current transients for both bearing combinations can be seen in Figures 9 and 10. By employing a slight overpotential on the working electrode (+50 mV vs. OCP) the resultant net anodic current flow between the working and reference electrodes is a measure of the depassivation and repassivation of the exposed surface. During sliding therefore, depassivation and accelerated corrosive degradation is observed as increased anodic current. By sampling the anodic current and load at a high frequency, it is possible to examine the depassivation of the surface as a result of interaction between the surfaces at the sliding interface over a cycle. The shape of current transients as well as current values varied over the course of the test. The transients displayed in Figures 9 and 10 represent typical shapes and values that were noted consistently over the full million cycles.

Clear periodicity, a repeating pattern in the anodic transient, was consistently noted across all tests; suggesting a link between the tribology and corrosive loss. Under standard gait a similar transient was seen for both metallic and ceramic acetabular components. A twin-peak current, similar to the loading profile was established. Both transients displayed a base level of current, 6 – 7 μA for MoM and 1 – 2 μA for MoC. Peaks in current were noted after unloading events, with the larger peak occurring after toe-off. Peaks in current of 11 μA were noted for MoM and 3 μA for MoC.

Under microseparation Metal-on-Metal bearings displayed peak currents of 100 μA and above after the second load peak (toe-off); an order of magnitude higher than standard gait. The current then decayed back down to a base level of approximately 10 μA with a slight peak before or upon the re-application of load. The shape of the Metal-on-Ceramic transient

was very different, with peaks occurring after toe-off and upon heel-strike. The larger of the peaks was also an order of magnitude higher than standard gait (approximately 40 μA) although occurred at heel strike. A base level current was also observed, although the decay to this base level was much more rapid than for MoM bearings.

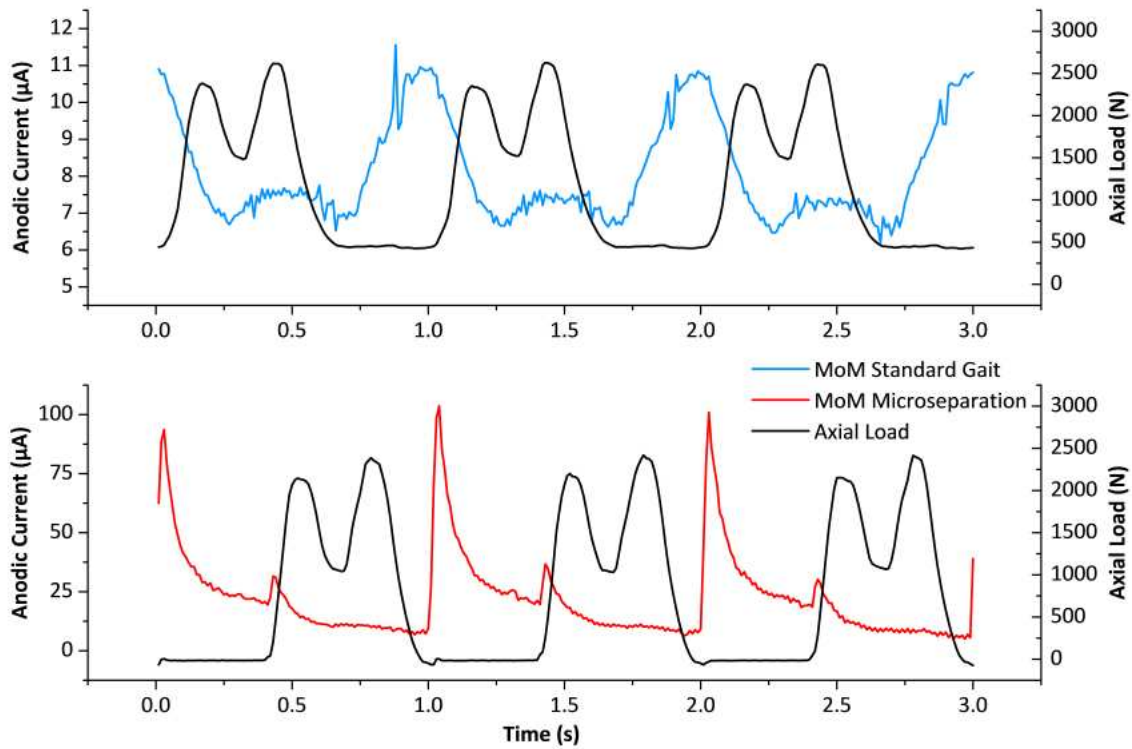


Figure 9 – Typical anodic current transients (+50 mV vs. OCP) for 28 mm MoM hip joints articulated at 1 Hz under Standard Gait (a) and Microseparation (b).

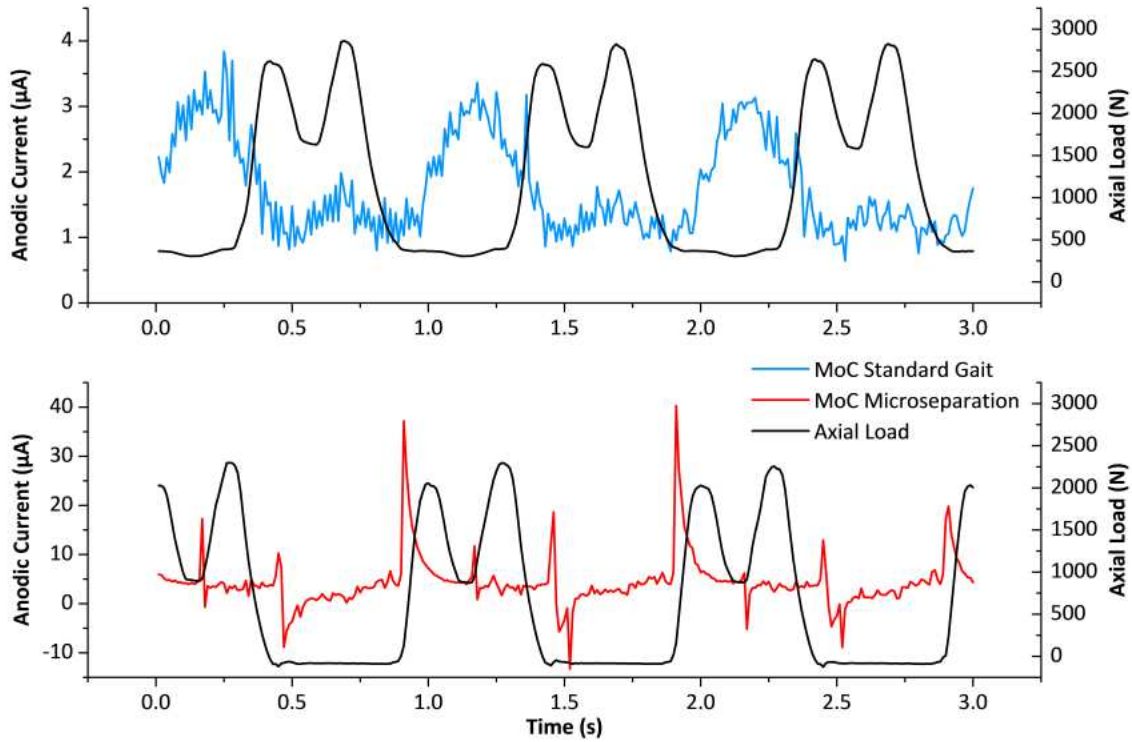


Figure 10 – Typical anodic current transients (+50 mV vs. OCP) for 28 mm MoC hip joints articulated at 1 Hz under Standard Gait (a) and Microseparation (b).

3.4. Total Material Loss

The results of the gravimetric analysis for the Metal-on-Ceramic femoral heads can be seen in Table 2. After one million cycles under Standard Gait gravimetric material loss of the femoral heads was recorded at 1.27 and 2.96 mg. For Microseparation mass losses of 6.09 and 4.40 mg were noted. A density of 8.29 g/cm³ for CoCrMo alloy was taken to convert values to volume losses [29]. Comparing the volume loss to the estimated corrosive loss it is possible to obtain values of 4.76 and 8.44 percentage corrosive loss under Standard Gait and as high as 17.7 percent under Microseparation. Due to an apparent electrode issue during the first 333,000 cycles for 'Microseparation 1' the final percentage value was not taken, although corrosive rates appeared similar over the remainder of the test. On the acetabular cup side, no significant material loss was noted for the ceramic cups. In two

cases, under both standard gait and microseparation, the ceramic inserts displayed a mass gain after one million cycles.

Table 2 – Gravimetric Mass Loss for 28 mm MoC Femoral Heads after one million cycles under Standard Gait and Microseparation

	Gravimetric Mass Loss (mg)	Volume (mm ³)	Estimated Corrosive Loss (mm ³)	Percentage Corrosion %
Standard Gait	1.27	0.154	0.013	8.44
	2.96	0.357	0.017	4.76
Microseparation	6.09	0.735	-	-
	4.40	0.531	0.094	17.70

Images produced by the form analysis software (RedLux Sphere Profiler) can be seen in Figure 11. Under standard gait a wear patch was noted slightly off centre on the pole of the femoral head due to the vertical orientation of the component in the ProSim Deep Flexion hip simulator. Under Microseparation a clear “stripe” was noted. After only 1 million cycles the analysis procedure of the RedLux software was not sufficient to accurately determine the small volume losses from the samples. The Standard Gait samples were estimated to have lost over twice as much as the Microseparation samples, contrary to the other techniques used. This technique may be more reliable for longer term tests with more clearly developed wear scars.

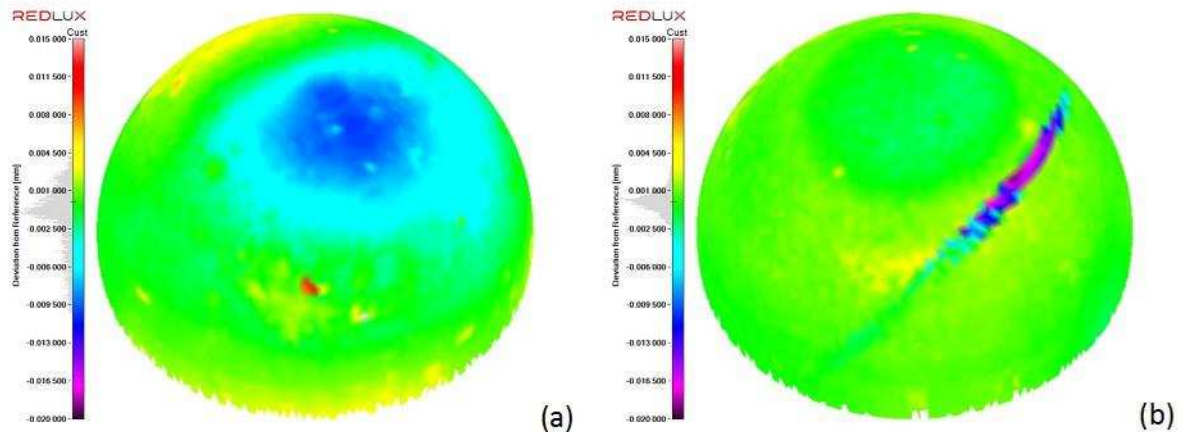


Figure 11 – Form Profile analysis for metallic Femoral Heads articulated against a ceramic counterface after one million cycles of Standard Gait (a) and Microseparation (b).

4. Discussion

4.1. *Standard Gait vs. Microseparation*

As discussed, the industry and research community are becoming increasingly interested in the effects of adverse loading situations and daily living activities on the performance of total hip replacements [23,24,30,31]. A continuous simple twin-peak profile may not be the best method for assessing these devices before they are implanted in patients. The use of a three electrode electrochemical cell in this study has highlighted how the pathways to material loss from the device may change by applying an adverse loading situation.

Moving from a Standard Gait profile to the application of 0.8 mm of Microseparation lead to differences in the OCP response and a significant increase in the estimated corrosive loss across both bearing couples. Comparing bearings in the Metal-on-Metal series, corrosive volume loss was estimated at as low as 0.029 mm³ under Standard Gait and 0.23-0.24 mm³ under Microseparation. This represents a near order of magnitude increase in the volume of corrosive material loss directly from the bearing surface. Under the MoC series similar

patterns were observed with increases from 0.013 and 0.017 mm³ to 0.09 mm³. The low value of 0.047 mm³ for the first MoC microseparated bearing is likely to be due to an electrode issue within the first 333,000 cycles, and thus the true material loss may have been higher.

Very few previous studies have examined the gravimetric material loss from 28 mm MoM bearings with the application of microseparation. One study demonstrated a non-significant increase in wear over the first million cycles [23]. After the initial bedding-in period the wear rate under microseparation increased, resulting in a 2.6 fold increase in total gravimetric material loss after five million cycles. Another study reported a three-to four fold increase over the first two million cycles, not separating the data for the initial million cycles [24]. These increases have previously been attributed to the breakdown of lubrication caused by the much more severe contact occurring at heel-strike, where the femoral head may also connect with the edge/rim of the acetabular cup [32]. Contact pressures as a result of a smaller 0.25 mm of microseparation have been estimated through modelling to be as high as 972 MPa for a 28 mm MoM bearing and 672 MPa for MoC [33,34]. The tribological contact is also likely to be very different, moving from Standard Gait sliding with sub-100 MPa contact pressures to more of a cutting action when meeting the rim under microseparation. This is highlighted with the typical 'stripe wear' pattern observed in Figure 11. This stripe pattern is typical of edge or rim loading and normally noted in Ceramic-on-Ceramic devices [35,36]. This action results in a more aggressive depassivation of the surface, as well as an increase in the generation of wear debris, resulting in a significantly higher rate of corrosion and therefore a higher rate of release of metallic ions directly at the bearing surface.

This is also demonstrated in the anodic current transients directly measured by applying a small overpotential to the bearing. On moving from Standard Gait to Microseparation, there is not only a change in the transient shapes for MoM and MoC, we also see an order of magnitude increase in peak currents.

The increase in the corrosive material loss represents a shift in the importance of corrosive degradation taking place at the bearing surface. As a result of moving from Standard Gait to Microseparation the estimated contribution of corrosion to the total material degradation moves from 4 – 8 % of the total to as much as 17 % for the Metal-on-Ceramic series. Even larger corrosive percentage contribution has been demonstrated under boundary lubricated contacts in simple reciprocating tribometer studies [37]. This shift is not captured by a simple gravimetric wear rate.

Saikko [30] demonstrated that under adverse loading conditions the gravimetric wear rate was not able to show a difference in performance of simulator tested hard-on-hard bearings unless the testing conditions passed a so-called 'endurance limit' for the device. de Villiers *et al.* [31] have also shown evidence of material degradation in hard-on-hard bearings with AgCrN coatings, despite no visible damage or gravimetric mass loss. Changes of the sliding regime to anything representing less than ideal conditions (i.e. adverse loading) could have large implications on the material degradation as a direct result of corrosion.

4.2. *Metal-on-Metal vs. Metal-on-Ceramic*

The use of Metal-on-Ceramic bearings has never been prevalent within the UK. Even following the rapid decline in Hard-on-Hard devices with a metal surface only 11 MoC devices were implanted in 2014 compared to 1,096 MoM devices [38]. The study of how this

contact behaves in a hip simulation may be useful however as the contact is simplified with only one active metallic surface. The large titanium acetabular shell is also removed from the electrochemical cell. A significant portion of tribometer studies rely on a ceramic counterface in order to study the depassivation of a single active metallic surface, and thus can be used to draw comparisons with the Metal-on-Ceramic series examined in the present study.

The Open Circuit Potential response of the Metal-on-Ceramic bearings for example was very different to the Metal-on-Metal series. Compared to the more typical response of an electrochemically instrumented sliding couple, the MoC series displayed an initial low OCP with a small cathodic shift upon the initiation of sliding. The OCP then displayed the same shift toward more noble values observed in the MoM bearings although was much more rapid. This is not a typical response seen in tribometer studies, which display sustained OCP drops on the initiation of sliding, despite being a similar material combination. This suggests the difference is system related which may have an impact on modern tribocorrosion models. These models have often been derived from base assumptions made for boundary lubricated tribometer contacts [39,40]. The model proposed by Cao *et al.* [41] for example predicts that both Metal-on-Metal and Metal-on-Ceramic spherical contacts within a hip simulator would display a degradation regime dominated by corrosive loss under a twin-peak profile. This does not appear to be the case in the present study, or for 36 mm diameter Metal-on-Metal contacts examined previously by Hesketh *et al.* [13].

The Metal-on-Ceramic series followed similar trends to the Metal-on-Metal series with significant increases in estimated corrosive material loss and in peak anodic currents under microseparation. The shape of the anodic currents changed under microseparation

however. Also overall the observed currents were lower for the MoC series. The lower currents may be explained simply by the fact that only one active surface is present in the contact. The values for corrosion current (I_{corr}) and the net anodic current transient are the overall currents measured through the electrochemical cell. With only one active surface the area of depassivated metal is less and there may have been similar current densities between the experiments. Differences in the tribological conditions may have also affected the corrosive degradation. Nominally, the contact between the two bearing combinations is similar, with similar values for radial clearance, initial surface roughness and thus lubrication regime. However the OCP trends for the MoM and MoC series, the latter of which did not display a typical cathodic tribocorrosion shift, suggests a difference in the effect of tribological conditions on the electrochemical cell. Further work is needed to elucidate these mechanisms.

Also of importance in the hip simulator cell is the presence of the titanium acetabular shell, which would not be a concern in the discussed tribometer studies. Under the Metal-on-Metal contact the sliding interface was electrically connected to the exposed surface of the titanium shell through the cup liner. This connection is not present for the Metal-on-Ceramic series as the ceramic liner insulated the metal femoral head from the shell. The MoM series therefore represents a mixed metal system, whereas the electrochemical analysis of the MoC series is purely concerned with the CoCrMo femoral head. Titanium is a much more noble metal than CoCrMo and connected to the sliding interface may polarise the depassivated wear scar, forming a galvanic cell and increasing corrosion. Bryant *et al.* [42] demonstrated this phenomena by utilising a titanium ring connected to the working electrode and exposed to the lubricant during fretting at the stem/cement interface. Of

importance is also the fact that the MoC series came from a different manufacturer and was a low carbon CoCrMo alloy.

5. Conclusions

- Under Microseparation the percentage contribution of electrochemical degradation to the total degradation of a metallic surface in a 28 mm diameter hip replacement was seen to increase.
- Both the corrosion current and anodic current transient measured during articulation for both Metal-on-Metal and Metal-on-Ceramic hip joints increased by approximately an order of magnitude under Microseparation conditions versus Standard Gait.
- Similar patterns in the anodic current transients for Metal-on-Metal and Metal-on-Ceramic hip joints under Standard Gait suggests a similar pathway to depassivation of the surface. The smaller currents measured for Metal-on-Ceramic may have been due to only one active surface in the interface.
- Adverse loading conditions may change the pathway of material loss during sliding for total joint replacements compared to Standard Gait simulation. For the success of the prosthesis, the dominating mechanism of loss needs further investigation.

The current use of pre-clinical simulator testing does not fully capture the degradation mechanisms of metallic surfaces in a sliding contact. Whilst great progress is being made to examine 'Adverse Loading' and 'Daily Living' scenarios, a simple gravimetric wear rate does

not distinguish their effect on corrosive material loss. The present study has demonstrated that moving to a microseparation loading profile greatly shifts the pathway to degradation, resulting in a greater percentage contribution of corrosion to total material loss. This may arguably be more important to the indications for revision commonly associated with MoM THR_s (ARMD, pseudotumor, high blood/urine ion levels) than the gravimetric wear rate. Tribocorrosion must be accounted for in pre-clinical assessment of new devices.

5. References

- [1] National Joint Registry. NJR 10th Annual Report for England, Wales and Northern Ireland. 2013.
- [2] Hart AJ, Quinn PD, Lali F, Sampson B, Skinner JA, Powell JJ, et al. Cobalt from metal-on-metal hip replacements may be the clinically relevant active agent responsible for periprosthetic tissue reactions. *Acta Biomater* 2012;8:3865–73.
- [3] Goldsmith AAJ, Dowson D. Development of a ten-station, multi-axis hip joint simulator. *Proc Inst Mech Eng H* 1999;213:311–6.
- [4] Anissian HL, Stark A, Gustafson A, Good V, Clarke IC. Metal-on-metal bearing in hip prosthesis generates 100-fold less wear debris than metal-on-polyethylene. *Acta Orthop Scand* 1999;70:578–82.
- [5] Goldsmith AAJ, Dowson D, Isaac GH, Lancaster JG. A comparative joint simulator study of the wear of metal-on-metal and alternative material combinations in hip replacements. *Proc Inst Mech Eng H* 2000;214:39–47.
- [6] Jin ZM, Firkins P, Farrar R, Fisher J. Analysis and modelling of wear of cobalt-chrome

- alloys in a pin-on-plate test for a metal-on-metal total hip replacement. *Proc Inst Mech Eng H* 2000;214:559–68.
- [7] Scholes SC, Green SM, Unsworth A. The wear of metal-on-metal total hip prostheses measured in a hip simulator. *Proc Inst Mech Eng H* 2001;215:523–30.
- [8] Firkins PJ, Tipper JL, Ingham E, Stone MH, Farrar R, Fisher J. Quantitative analysis of wear debris from metal on metal hip prostheses tested in a physiological hip joint simulator. 45th ORS Annu. Meet., California, USA: 1999.
- [9] Yan Y, Neville A, Dowson D, Williams S, Fisher J. The influence of swing phase load on the electrochemical response, friction, and ion release of metal-on-metal hip prostheses in a friction simulator. *Proc Inst Mech Eng J* 2009;223:303–9.
- [10] Yan Y, Neville A, Dowson D, Williams S, Fisher J. Electrochemical instrumentation of a hip simulator: a new tool for assessing the role of corrosion in metal-on-metal hip joints. *Proc Inst Mech Eng H* 2010;224:1267–73.
- [11] Yan Y, Dowson D, Neville A. In-situ electrochemical study of interaction of tribology and corrosion in artificial hip prosthesis simulators. *J Mech Behav Biomed Mater* 2013;18:191–9.
- [12] Hesketh J, Meng Q, Dowson D, Neville A. Biotribocorrosion of metal-on-metal hip replacements: How surface degradation can influence metal ion formation. *Tribol Int* 2013;65:128–37.
- [13] Hesketh J, Hu X, Yan Y, Dowson D, Neville A. Biotribocorrosion: Some electrochemical observations from an instrumented hip joint simulator. *Tribol Int* 2013;59:332–8.
- [14] Macdonald DD, Urquidi-Macdonald M. Theory of Steady-State Passive Films. *J*

- Electrochem Soc 1990;137:2395–402.
- [15] Watson SW, Friedersdorf FJ, Madsen BW, Cramer SD. Methods of Measuring Wear-Corrosion Synergism. *Wear* 1995;181-183:476–84.
- [16] Hesketh J, Ward M, Dowson D, Neville A. The composition of tribofilms produced on metal-on-metal hip bearings. *Biomaterials* 2014;35:2113–9.
- [17] Bryant M, Farrar R, Brummitt K, Freeman R, Neville A. Fretting corrosion of fully cemented polished collarless tapered stems: The influence of PMMA bone cement. *Wear* 2013;301:290–9.
- [18] Yan Y, Neville A, Dowson D. Biotribocorrosion of CoCrMo orthopaedic implant materials—Assessing the formation and effect of the biofilm. *Tribol Int* 2007;40:1492–9.
- [19] Wimmer MA, Mathew MT, Laurent MP, Nagelli C, Liao Y, Marks LD, et al. Tribochemical Reactions in Metal-on-Metal Hip Joints Influence Wear and Corrosion 2013:292–309.
- [20] Meyer JN, Mathew MT, Wimmer MA, LeSuer RJ. Effect of tribolayer formation on corrosion of CoCrMo alloys investigated using scanning electrochemical microscopy. *Anal Chem* 2013;85:7159–66.
- [21] Wimmer MA, Fischer A, Buscher R, Pourzal R, Sprecher C, Hauert R, et al. Wear mechanisms in metal-on-metal bearings: the importance of tribochemical reaction layers. *J Orthop Res* 2010;28:436–43.
- [22] International Standards Organisation. BS ISO 14242-1:2014 - Implants for surgery - Wear of total hip-joint prostheses - Part 1: Loading and displacement parameters for

- wear-testing machines and corresponding environmental conditions for test 2014.
- [23] Williams S, Leslie I, Isaac G, Jin Z, Ingham E, Fisher J. Tribology and wear of metal-on-metal hip prostheses: influence of cup angle and head position. *JBJSAm* 2008;90 Suppl 3:111–7.
- [24] Al-Hajjar M, Williams S, Fisher J, Jennings LM, Lim CT, Goh JCH. The Influence of Cup Inclination Angle and Head Position on the Wear of Metalon-Metal Bearings in Total Hip Replacements. 6th World Congr. Biomech. 31st ed., Singapore: 2010, p. 752–5.
- [25] International Standards Organisation. BS ISO 14243-3:2004 - Implants for surgery - Wear of total knee-joint prostheses - Part 3: Loading and displacement parameters for wear-testing machines with displacement control and corresponding environmental conditions for test 2004.
- [26] Stern M, Geary AL. Electrochemical Polarization: I. A Theoretical Analysis of the Shape of Polarization Curves. *J Electrochem Soc* 1957;104:56–63.
- [27] Hesketh J, Hu X, Dowson D, Neville A. Tribocorrosion reactions between metal-on-metal and metal-on-polymer surfaces for total hip replacement. *Proc Inst Mech Eng J* 2012;226:564–74.
- [28] International Standards Organisation. BS ISO 14242-2:2000 - Implants for surgery - Wear of total hip-joint prostheses - Part 1: Loading and displacement parameters for wear-testing machines and corresponding environmental conditions for test 2000.
- [29] 3T RPD. Material Specification: Cobalt Chrome Alloy Co28Cr6Mo n.d.
- [30] Saikko V. Effect of increased load on the wear of a large diameter metal-on-metal modular hip prosthesis with a high inclination angle of the acetabular cup. *Tribol Int*

- 2016;96:149–54.
- [31] de Villiers D, Shelton JC. Measurement outcomes from hip simulators. *Proc Inst Mech Eng H* 2016;230:398–05.
- [32] Fisher J. Bioengineering reasons for the failure of metal-on-metal hip prostheses: an engineer’s perspective. *JBSBr* 2011;93:1001–4.
- [33] Wang L, Liu X, Li D, Liu F, Jin Z. Contact mechanics studies of an ellipsoidal contact bearing surface of metal-on-metal hip prostheses under micro-lateralization. *Med Eng Phys* 2014;36:419–24.
- [34] Mak M, Jin ZM, Fisher J, Stewart TD. Influence of acetabular cup rim design on the contact stress during edge loading in ceramic-on-ceramic hip prostheses. *J Arthroplast* 2011;26:131–6.
- [35] Walter WL, Insley GM, Walter WK, Tuke MA. Edge loading in third generation alumina ceramic-on-ceramic bearings: Stripe wear. *J Arthroplast* 2004;19:402–13.
- [36] Al-Hajjar M, Fisher J, Tipper JL, Williams S, Jennings LM. Wear of 36-mm BIOLOX(R) delta ceramic-on-ceramic bearing in total hip replacements under edge loading conditions. *Proc Inst Mech Eng H* 2013;227:535–42.
- [37] Hesketh J. Tribocorrosion of Total Hip Replacements. University of Leeds, 2012.
- [38] National Joint Registry. 12th Annual Report: Prostheses used in hip, knee, ankle, elbow and shoulder replacement procedures 2014. 2015.
- [39] Papageorgiou N, Mischler S. Electrochemical Simulation of the Current and Potential Response in Sliding Tribocorrosion. *Tribol Lett* 2012;48:271–83.
- [40] Vieira AC, Rocha LA, Papageorgiou N, Mischler S. Mechanical and electrochemical

deterioration mechanisms in the tribocorrosion of Al alloys in NaCl and in NaNO₃ solutions. *Corros Sci* 2012;54:26–35.

[41] Cao S, Guadalupe Maldonado S, Mischler S. Tribocorrosion of passive metals in the mixed lubrication regime: theoretical model and application to metal-on-metal artificial hip joints. *Wear* 2015;324–325:55–63.

[42] Bryant M, Farrar R, Freeman R, Brummitt K, Nolan J, Neville A. Galvanically enhanced fretting-crevice corrosion of cemented femoral stems. *J Mech Behav Biomed Mater* 2014;40:275–86.